Matrix metallopeptidase 9 targeted by hsa-miR-494 promotes silybin-inhibited osteosarcoma

Tianhao Sun [1], Kelvin S. C. Cheung [1], Zhi-Li Liu [2*], Frankie Leung [1,3*], and William W. Lu [1*]

[1] Department of Orthopaedics and Traumatology, Li Ka Shing Faculty of Medicine, The University of Hong Kong, Hong Kong SAR, China

[2] Department of Orthopedic Surgery, the First Affiliated Hospital of Nanchang University, Nanchang, China

[3] Shenzhen Key Laboratory for Innovative Technology in Orthopaedic Trauma, Department of Orthopaedics and Traumatology, The University of Hong Kong-Shenzhen Hospital, Shenzhen, China

* To whom correspondence should be addressed. Tel: +852-3917-9595 (William W. Lu); Fax: +852-2818-5210 (William W. Lu); Email: wwlu@hku.hk (William W. Lu); Email: klleunga@hku.hk (Frankie Leung); Email: sunmishu@126.com (Zhi-Li Liu)

Acknowledgements

The work described on this paper was substantially supported by grants from the HK RGC (Ref No. T13-402/17-N), Strategic Research Theme of Biomedical Engineering and Nanotechnology, Shenzhen Science and Technology Funding (Ref No. JCYJ20160429185449249), and Guangdong Scientific Plan (Ref No. 2014A030313743).

Abbreviations

osteosarcoma (OS)

matrix metallopeptidase 9 (MMP-9)

Runt-related transcription factor 2 (RUNX2)

Short Tandem Repeat (STR)

immunocytochemistry (ICC)

MicroRNAs (miRNAs)

Epithelial-to-mesenchymal transition (EMT)

Proliferating Cell Nuclear Antigen (PCNA)

Poly(ADP-Ribose) Polymerase 1 (PARP1)

Abbreviated Title

MMP-9 promotes osteosarcoma

Keywords: MMP-9; MiR-494; Silybin; Osteosarcoma; Cell proliferation

Abstract

Osteosarcoma (OS) is the most common malignant tumor that develops in bone. Its mortality is very high. Therefore, study of mechanisms of pathogenesis of the OS is urgently required. Previous studies of microarray showed that the expression levels of matrix metallopeptidase 9 (MMP-9) altered significantly in OS. In addition, overexpression of MMP-9 is recognized as an indicator in cancer. However, the exact roles of MMP-9 in OS are not fully investigated. Thus, we firstly studied the roles of MMP-9 in OS and revealed that silence of MMP-9 inhibited OS cell proliferation as determined by MTT assay and colony formation assay. Secondly, we conducted TUNEL assay and confirmed loss of functions of MMP-9 induced OS cell apoptosis. Next, we used lentivector packaging method to overexpress MMP-9 and found that overexpression of MMP-9 promoted OS cell migration. Fourthly, the results of luciferase assay showed that MMP-9 was targeted by hsa-miR-494, which inhibited OS. Fifthly, we revealed that the levels of hsa-miR-494 were upregulated by the drug silybin which inhibited OS. Finally, we revealed that silybin inhibited OS cell viability by altering the protein levels of β-catenin and Runt-related transcription factor 2 (RUNX2) as determined by western blot and immunocytochemistry (ICC).

Introduction

OS is the most common cancer in the bone. OS tends to metastasize and recur because it commonly occurs where rich blood supplies [1]. The survival rate for these patients with recurrent disease is less than 30% [2]. Thus, study of pathogenesis of the OS and novel agents used for treating OS are urgently required [3]. Results of the ectopic expression of genes produced by microarray showed that the levels of MMP-9 was differentially expressed gene in OS compared with its controls [4]. Thus, we hypothesized that the MMP-9 might play important roles in OS. There are several studies of the roles of MMP-9 in breast cancer [5], but the studies of its exact roles in OS are very few.

MicroRNAs (miRNAs) are small non-coding RNA and induce gene silencing by binding to their target mRNAs [6]. For instance, our previous studies found that miR-375-3p negatively regulated osteogenesis by targeting β-catenin [7]. miRNAs regulate substantial biological procedures such as cell cycle, cell differentiation and cell apoptosis. For example, our previous data showed that miR-9-5p decreased the mouse cell line MC3T3-E1 cell proliferation and cell adhesion [8]. miRNAs can be used as biomarkers for diagnosing diseases and potential therapeutic reagents [9]. They play vital roles in cancer including OS. Epithelial-to-mesenchymal transition (EMT) means the transition of epithelial cells to mesenchymal cells, which is the indication of cancer. Vimentin is one of the most important biomarker of EMT. The decline of vimentin suggests inhibition of tumor [10].

The expression levels of miRNAs and their targets are regulated by compounds and drugs. The drugs exert their effects such as anticancer effects by regulating the levels of miRNAs. Silybin (also known as silibinin) is a compound extracted from a natural herb, and it is used as

the drug treating tumors such as hepatocellular carcinoma [11] and liver diseases [12]. Previous studies showed that silybin inhibited OS MG-63 cell invasion by inhibiting the c-Jun/AP-1 induction of MMP-2 [13]. However, the exact roles of silybin in OS such as cell proliferation are not well studied.

Wnt signaling pathways including β-catenin are essential for carcinogenesis. Previous studies showed that WNT/β-catenin signaling modulated RUNX2 [14,15]. RUNX2 was the upstream regulator of MMP-9 [16]. The roles of β-catenin and RUNX2 in tumorigenesis are not fully clear. Some studies found that β-catenin expression increased while other studies suggested that β-catenin expression was reduced in cancer [17]. Therefore, to study the expression of β-catenin/RUNX2 signaling in tumor especially in OS is meaningful because RUNX2 is extensively expressed in bone tissues.

In the present study, we aim to explore the roles of the MMP-9, miRNA and silybin in OS and their regulatory relationships. These findings might provide supports for MMP-9 and miRNA as the potential therapeutic targets. The potential use of silybin as the drugs for OS was also explored.

Materials and Methods

Cell culture and reagents

MG-63 cells were cultured in Minimum Essential Medium Eagle (Sigma-Aldrich) supplemented with 10% FBS and antibiotics. Saos-2 cells were cultured in McCOY'S 5A Medium (Sigma-Aldrich) supplemented with 10% FBS and antibiotics. 293FT cells were cultured in DMEM (Sigma-Aldrich) supplemented with 10% FBS and antibiotics. Silybin

(CAS No. 22888-70-6) was purchased from Sigma-Aldrich. For miRNA mimics and siRNA transfection, we used 0.5% HiPerfect (Qiagen). For luciferase reporter assay, cells were co-transfected with plasmids and miRNA mimics in the presence of Lipofectamine 2000. The human siRNA siMMP-9 was purchased from Life Technologies Limited (ThermoFisher Scientific). The MG-63 and Saos-2 cells were obtained from the Orthopaedic Research Centre, The University of Hong Kong. All the cell lines have been authenticated morphologic observation. .

Short Tandem Repeat (STR) Profiling

After DNA extraction, we conducted PCR by using GeneAmp® PCR system9700 (ABI3730XL), mixed the PCR products, STR-500 and HIDI reagents. Amplified products were separated using an Applied Biosystems 3737XL Genetic Analyzer. We referred to ANSI/ATCC Authentication of Human Cell Line Standardization of STR Profiling 2011, ASN-0002-2011 and compared the results of our cells with standards through DSMZ database. More than 80% of STR matching rate was considered as the same sources of cells.

Transfection

We used three ways to transfect. Firstly, for transfection of smaller molecules such as silence RNA (siMMP-9) and miRNA (hsa-miR-494) mimics and inhibitors, we used HiPerfect (Qiagen) as the transfection reagent. In brief, we added HiPerFect to the medium without serum and gave a final HiPerFect concentration of 0.5% (v/v) after adding cells. We diluted siRNA or miRNAs mimics/inhibitors in aforementioned medium, mixed, incubated for 10 minutes at room

temperature, and added the cells. Secondly, for transfection or co-transfection of larger molecules such as plasmids (constructs of 3'UTR of MMP-9), we used Lipofectamine 2000 (Thermo Fisher Scientific) as the transfection reagent. In this case, we added Lipofectamine 2000 to the medium without serum and gave a final concentration of 0.33% (v/v) after adding cells. Then we mixed and incubated for 5 min at room temperature. We diluted miRNAs (hsa-miR-494) mimics and plasmids (wild type or mutant constructs of 3'UTR of MMP-9) in medium without serum, mixed with the aforementioned medium containing Lipofectamine 2000, incubated for 20 minutes at room temperature, and added the cells. Thirdly, for transfection of our constructed lentivector plus pPACK (System Biosciences) packaging mix, we used PureFection (System Biosciences) as the transfection reagent. In brief, 24 hours prior to transfection, we seeded 293FT cells in medium without antibiotics, then added pPACKH1 and our lentivector constructs into serum free medium, mixed, added PureFection into the same tube and incubated at room temperature for 15 minutes, and finally added the mixture to the cells.

MTT cell proliferation assay

We added siMMP-9 with transfection reagent HiPerfect (Qiagen) into the medium without FBS and antibiotics. This mixture was incubated for 10 min at room temperature. We seeded cells at a concentration of 5×10^4 cells/well in total 150 μL culture medium with FBS and antibiotics containing various amounts of siMMP-9 into 96 wells microplates. Cell viability was checked after 24, 48, and 72 hours of transfection. We conducted this assay by using Cell Growth Determination Kit MTT Based (Sigma-Aldrich). In brief, we added 5mg/ml MTT without

phenol red in an amount equal to 10% of the culture volume (15 μL), incubated for 3 hours, removed the culture fluid, dissolved the resulting MTT formazan crystals by adding 0.1 N HCl in isopropanol, mixed and spectrophotometrically measured absorbance at a wavelength of 570 nm, and subtracted background absorbance measured at 690 nm. All the wells were quadruple repetitions. Every four wells in 96 wells microplates were manipulated in the same way with the same concentrations of siMMP-9 (or their controls). For each independent experiment, three 96 wells microplates were used for detection of Day 1, Day 2 and Day 3 respectively.

XTT cell proliferation assay

We conducted this assay by using Cell Proliferation Kit II (XTT) (Roche). In brief, we added XTT labeling mixture, incubated for 4h, and measured absorbance at 475 nm, and the reference wavelength was 660 nm by spectrophotometer.

Colony formation assay

Colony formation assay was used for detection of the effects of siMMP-9 or silybin on cell proliferation. To test the influences of siMMP-9 on cell growth, we added HiPerFect to the medium without serum, mixed, added siMMP-9 (2.5 nM), mixed, incubated for 10 minutes at room temperature, and added the MG-63 and Saos-2 cells. For the detection of effects of silybin on cell viability, the seeded cells were treated with different concentrations of silybin (20 μM and 80 μM). We seeded cells at a concentration of 2000 cells/well in total 1.5 ml culture medium into 6 wells plates. Seven days after transfection, the cells were proceeded. The cell culture medium was removed and the cells were rinsed with PBS. The cells were fixed by 70% ethanol

for 30 mins and stained by 0.5% crystal violet (Sigma-Aldrich) for one hour. Then we removed the glutaraldehyde crystal violet carefully and sank and rinsed with water. We leaved the plates to dry and then counted the colonies.

TUNEL cell apoptosis assay

ApopTag® Red In Situ Apoptosis Detection Kit (Merck Millipore Corporation) was used in cell apoptosis assay. It utilized an anti-digoxigenin antibody with a rhodamine fluorochrome. We seeded cells at a concentration of 1×10^4 cells/well in total 150 μl medium into 12 wells chamber (ibidi, Martinsried, Germany). The siMMP-9 was transfected into the cells and the transfection duration was 48 hours. It was fixed in 1% paraformaldehyde, sequentially applied with Equilibration Buffer, TdT Enzyme, Stop/Wash Buffer, Anti-Digoxigenin Conjugate and Rhodamine/DAPI Staining. When taking photos, we assured consistent parameters of the fluorescence microscopy for each picture so that all the pictures were comparable.

Establishment of stable cell line overexpressing MMP-9

This part included two main steps. The first step was to generate expression constructs of MMP-9 in the pCDH cDNA Cloning and Expression Lentivectors (System Biosciences). The second step was to package the pCDH expression constructs into pseudotyped viral particles and transduce the target cells with these particles.

Firstly, we used Human MMP-9 Gene cDNA clone plasmid (Sino Biological Inc.) which contained the full length of human MMP-9 gene (NM_004994.2) as the PCR template. We amplified the MMP-9 by PCR in which the Phusion® High-Fidelity DNA Polymerase (New

England Biolabs) was used. The PCR products were purified and digested with EcoRI and NotI. The vector pCDH-CMV-MCS-EF1-GreenPuro cDNA Cloning and Expression Vector (System Biosciences) was digested and purified for ligation. The competent cells were DH5α and ampicillin plates were used for selection. Colony PCR and sequencing were used for verification of the final expression constructs. The sequences of primers used for sequencing was 5'-CACGCTGTTTTGACCTCCATAGA-3'.

To make lentivirus, we co-transfected our constructed lentivector plus pPACK (System Biosciences) packaging mix using PureFection (System Biosciences) into 293FT cells. After 48 hours, we collected supernatant and combined with PEG-it virus concentration solution (System Biosciences). Next day, we removed supernatant and resuspended pellet in PBS. Then we combined the virus with TransDux (System Biosciences) and infected our target cells. Puromycin (Santa Cruz) was used to select for stably transduced cells.

qPCR detection of mRNA and miRNA

TRIzol was used for RNA extraction. For each well of 6 well plate, 1 ml TRIzol was added. NanoDrop was used to detect RNA concentration. The same amount of RNA was used for all the samples. For detection of levels of miRNAs, the RNA was polyadenylated by Poly (A) Polymerase Tailing Kit (Epicentre® Biotechnologies) before reverse transcription. Reverse transcription included two ways. One was for mRNA detection and the other was for miRNA detection. For mRNA detection, random primer was used. For miRNA detection, designed primer was used and its sequence was 5'-GCGAGCACAGAATTAATACGACTCACTATAGGTTTTTTTTTTAG-3'. Diluted cDNA

was used for qPCR. The master mix was SYBR Green (Applied Biosystems). Each cDNA sample was triplicate in 96 well plate. Data were analyzed using the $2^{-\Delta\Delta CT}$ relative quantification method. The sequences of primers were listed in the Table 1. All the primers were verified by Primer-BLAST (NCBI). GAPDH and U6 were the internal control for mRNA and miRNA respectively.

hsa-miR-494-pmirGLO plasmid construction and luciferase reporter assays

First, we designed sequences including the two sequences of MMP-9. The sequences were synthesized as the oligonucleotides. Then the forward and reverse ones were made into double strand DNA fragments. Then we ligated the DNA fragments into the pmirGLO Dual-Luciferase miRNA Target Expression Vector (Promega) digested with SacI and XhoI. Colony PCR, agarose gel electrophoresis and sequencing confirmed the ligation was successful. Thus, we successfully inserted the wild type and mutant fragments of the 3'UTR of MMP-9 containing the binding sites of hsa-miR-494 into the luciferase vector. We co-transfected the MG-63 cells with the plasmids and hsa-miR-494 mimics (Exiqon), whose sequence was 5'-TGAAACATACACGGGAAACCTC-3'. We used Dual-Glo® Luciferase Assay System (Promega) for measuring firefly luciferase activities 48 h after transfection. In brief, we measured firefly luciferase activity by adding Dual-Glo® Luciferase Reagent into the cell medium. The firefly luminescence was firstly measured. Then we measured Renilla luciferase activity by adding Dual-Glo® Stop & Glo Reagent into the original culture medium. Renilla luminescence was measured in the same plate order as the firefly luminescence was measured. Then we calculated the ratio of luminescence from the experimental reporter (firefly) to

luminescence from the control reporter (Renilla), normalized this ratio to the ratio of control wells.

Western Blot

Western blotting analysis was performed with the standard protocol. In brief, the MG-63 or Saos-2 cells were seeded in 6 well plate (5×10^5 cells/well). The cells were treated with a serial dilution of silybin and DMSO as the control. The lysis buffer was Radio Immunoprecipitation Assay (RIPA) buffer with SIGMAFAST Protease Inhibitor Cocktail Tablets (Sigma). The Laemmli buffer was used to denature the samples. The PVDF membrane was blocked by 5% BSA solution for one hour. Primary antibodies included Anti-beta catenin antibody (Abcam), Anti-Runx2 antibody (Abcam), Anti-Vimentin antibody (Abcam), Anti-PCNA antibody (Abcam), Anti-PARP1 antibody (Abcam), Anti-Cytochrome C antibody (Abcam), Anti-beta actin antibody (Sigma), and Anti-caspase-3 (Cell Signaling Technology). Secondary antibodies included Goat Anti-Rabbit IgG H&L (HRP) (Abcam) and Rabbit Anti-Mouse IgG H&L (HRP) (Abcam). For beta actin staining, the membrane was incubated with the first antibody (1:10000 dilution) for one hour at room temperature, rinsed with TBST, and then incubated with the second antibody (1:50000 dilution) for one hour at room temperature. For all the other staining, the membrane was incubated with the first antibody overnight at 4℃, rinsed with TBST, and then incubated with the second antibody (1:2000 dilution) for one hour at room temperature. The dilution of Anti-beta catenin antibody was 1:4000 and the dilution of all the other primary antibodies was 1:1000. ECL Prime Western Blotting Reagents (GE Healthcare) were used to develop. The developer was myECL Imager (Thermo Fisher Scientific).

ICC and Immunofluorescence (IF)

The expression levels of RUNX2 were detected by ICC and IF. We seeded cells at a concentration of 1×10^4 cells/well in total 150 μl medium into 12 wells chamber (ibidi, Martinsried, Germany) and treated the cells with silybin (10 μM). DMSO was used as the control. The duration of treatment was one day. The cells were fixed with 4% paraformaldehyde in PBS, permeabilized with 0.1% Triton X-100, blocked with 10% Normal Goat Serum (Life Technologies), incubated with primary antibody RUNX2 Antibody (Abcam) at a 1/1000 dilution overnight, and then secondary antibody Goat Anti-Rabbit Ig G (Alexa Fluor 488) (Abcam) at a 1/200 dilution. The intensity of fluorescence was quantified by the software ImageJ. In brief, the optical density was calibrated. The thresholds of all the pictures were comparably adjusted. The relative intensity was calculated as Integrated Density/Area (limit to threshold). The experimental groups were normalized to their controls.

Statistical Analysis

Statistical analysis was performed by a t-test or paired t-test, and $p<0.05$ was considered statistically significant. The software GraphPad Prism was used to draw the charts.

Results

Cell authentication of MG-63 and Saos-2

To discriminate species, confirm identity, and detect cell cross-contamination, we conducted STR Profiling [18,19]. The results showed that the information of our cell samples of MG-63

and Saos-2 was in accordance with that of standard cell bank (Table 2 and supplement Fig. S1 and Fig. S2).

Silence of MMP-9 inhibited OS

We silenced the functions of MMP-9 in two OS cell lines (MG-63 and Saos-2) by using siMMP-9. Results of MTT-based colorimetric assay showed that siMMP-9 inhibited both MG-63 and Saos-2 cell proliferation in a dose dependent manner (Fig. 1a, 1b). Colony formation assay also showed that both the number and size of cell colonies of MG-63 and Saos-2 (blue dots) decreased after the cells were treated with siMMP-9 (Fig. 1c, 1d, 1e, 1f). In addition, we also detected the levels of a cell proliferation biomarker Proliferating Cell Nuclear Antigen (PCNA), and found both mRNA and protein levels of PCNA decreased after the MG-63 and Saos-2 cells were transfected with siMMP-9 (Fig. 1g, 1h, 1i). Taken together, all these data suggested that loss of functions of MMP-9 in OS cell line suppressed cell proliferation, indicating that the silence of MMP-9 inhibited OS carcinogenesis.

Silence of MMP-9 induced OS cell apoptosis

Since our results showed siMMP-9 inhibited cell proliferation, we then detected whether it induced cell apoptosis. Results showed that siMMP-9 increased the levels of Poly(ADP-Ribose) Polymerase 1 (PARP1) and Cytochrome C, the indicators of apoptosis, as determined by Western Blot (Fig. 2a), indicating siMMP-9 promoted OS cell apoptosis. We then further confirmed silence of MMP-9 induced OS cell apoptosis by conducting TUNEL assay. Results showed that siMMP-9 induced MG-63 cell apoptosis in a dose dependent manner (Fig. 2b, 2c).

Overexpression of MMP-9 promoted OS cell migration

To further verify the effects of MMP-9 on carcinogenesis, we overexpressed MMP-9 and established stable cell line by using plasmid construction and lentivector packaging method. Firstly, we studied whether the transduced cells could stably overexpress MMP-9. qPCR results showed that the expression levels of MMP-9 in transduced cells were significantly higher than the normal cells (Fig. 3a), suggesting that we have successfully overexpressed MMP-9 in Saos-2 cells. We found that the pseudopods (also called pseudopodia) of transduced cells overexpressing MMP-9 were much longer and more significant than the normal cells (Fig. 3b). Protrusion of cell pseudopod is an important element of cell migration and therefore of tumor cell metastasis and invasion [20]. Thus, the Saos-2 cells overexpressing MMP-9 might be more invasive and malignant than their controls.

MMP-9 was targeted by hsa-miR-494 which inhibited OS

Based on MMP-9, we then further studied its upstream regulatory miRNAs. Prediction tool microRNA.org-Targets and Expression (http://www.microrna.org/microrna/home.do) showed that hsa-miR-494 was the miRNA regulating MMP-9 (Fig. 4a). Fig. 4a showed the binding sites between the hsa-miR-494 and 3'UTR of MMP-9. To confirm the specific binding relationship, we also generated mutant sites in the 3'UTR of MMP-9 (Fig. 4a). Results of luciferase assay confirmed the binding. Specifically, in hsa-miR-494 mimics-treated MG-63 cells, the luciferase activity of cells transfected with wild type MMP-9 plasmids decreased while that of mutant MMP-9 plasmids was not significantly changed (Fig. 4b). In other words, transfection of hsa-miR-494 mimics resulted in a significant reduction in luciferase activity in cells transfected

with wild type plasmids, while this inhibition of luciferase activity by hsa-miR-494 was abrogated in cells transfected with mutant plasmids (Fig. 4b). Finally, we tested the effects of hsa-miR-494 on OS cell proliferation. Transfection of hsa-miR-494 inhibitors increased the cell proliferation rate of MG-63 and Saos-2 cells (Fig. 4c, 4d), indicating that hsa-miR-494 might decrease OS cell viability. The results of Western Blot also showed hsa-miR-494 mimics increased the levels of caspase-3 while hsa-miR-494 inhibitors decreased caspase-3 (Fig. 4e), indicating that hsa-miR-494 induced OS cell apoptosis. To further explore the mechanisms of hsa-miR-494 inhibiting cancer, we detected the expression of β-catenin/RUNX2/vimentin signal because of three reasons. The first reason was that β-catenin and RUNX2 played vital roles in tumorigenesis [21,22]. The second reason was that β-catenin/RUNX2 regulated the expression of vimentin [23],[24]. The third reason was vimentin was the important biomarker of EMT. Western blot showed that hsa-miR-494 mimics decreased the levels of β-catenin, increased the levels of RUNX2, and decreased vimentin (Fig. 4f), suggesting that hsa-miR-494 inhibited EMT and cancer by regulating β-catenin/RUNX2 signal.

Hsa-miR-494 were upregulated by silybin which inhibited OS

Based on hsa-miR-494, we then tried to find drugs used for treating OS. Previous studies showed that hsa-miR-494 was regulated by silybin in head and neck squamous cell carcinomas [25]. Thus, we firstly studied whether the expression levels of hsa-miR-494 could be altered by silybin in OS. Results showed that silybin increased the levels of hsa-miR-494 in a dose dependent manner in Saos-2 cells (Fig. 5a). Next, we used colony formation assay to investigate the effects of silybin on cell proliferation, and results showed silybin inhibited OS cell viability

in a dose dependent manner in both MG-63 and Saos-2 cells (Fig. 5b, 5c, 5d). To further confirm the results of colony formation, we conducted XTT-based colorimetric assay. Results showed the cell proliferation of the two OS cell lines (MG-63 and Saos-2) were suppressed by silybin in a dose dependent manner (Fig. 5e, 5f).

Silybin modulated the protein levels of β-catenin and RUNX2

To further explore the mechanisms of the effects of silybin on cancer, we detected the protein levels of β-catenin and RUNX2 because MMP-9 was regulated by the β-catenin/RUNX2 signal. Interestingly, the silybin altered the levels of β-catenin and RUNX2 in reversed ways in MG-63 and Saos-2 cells. Specifically, silybin increased the protein levels of β-catenin and decreased the levels of RUNX2 in MG-63 cells (Fig. 6a). In contrast, the results were reversed for Saos-2 cells (Fig. 6a). These results suggested that silybin might suppress the OS carcinogenesis via different ways. However, there were consistent results for these two cells. After treatment of silybin, the changes of levels of β-catenin and RUNX2 were reversed in both MG-63 and Saos-2 cells, indicating that β-catenin might negatively regulate RUNX2. To further confirm our results, we conducted immunocytochemistry. After treatment of silybin, the cells were greener. In other words, the degree of green was higher in the silybin-treated group than the control group, suggesting that the protein levels of RUNX2 in Saos-2 cells increased after the cells were treated with silybin (Fig. 6b, 6c), which confirmed the western blot results.

Discussion

In our present study, we revealed that silence of MMP-9 suppressed OS cell proliferation and

induced cell apoptosis, indicating that MMP-9 promoted tumorigenesis. Then we revealed that MMP-9 was targeted and negatively regulated by hsa-miR-494 which inhibited cell proliferation, indicating that hsa-miR-494 might suppress OS. Finally, we found that the drug silybin could upregulate hsa-miR-494 and arrest carcinogenesis by inhibiting cell proliferation. Al these relationships are summarized in the Supplementary Fig. 7.

Although MMP-9 was reported as a potential biomarker for diagnosing OS, more investigations were undoubtedly needed to confirm its diagnostic value [26]. In this study, we revealed that MMP-9 might promote tumorigenesis, which provided more evidences to support MMP-9 as the biomarker for OS. Several studies linked elevated MMP-9 expression to increased tumor stage [27]. Our results were consistent with these studies because we pointed out that loss of functions of MMP-9 suppressed tumor. In the present study, we revealed that siMMP-9 decreased OS cell proliferation and increased cell apoptosis at the same time. The effects of MMP-9 on OS cell proliferation and apoptosis are synergetic, indicating that MMP-9 might strongly promote carcinogenesis.

Based on MMP-9, we further studied its regulatory miRNA hsa-miR-494 because the miRNA was predicted by the miRNA prediction tool. Another reason that we selected to study hsa-miR-494 was that it was reported to act as an anti-oncogene in gastric carcinoma [28], esophageal squamous cell carcinoma [29], oral cancer [30], and breast cancer [31]. All these studied suggested that miR-494 might be a tumor suppressor. Our study also showed that hsa-miR-494 suppressed OS cell proliferation. However, there are a few contrary reports. For example, a study reported that miR-494 promoted cell proliferation and increased sorafenib resistance in hepatocellular carcinoma [32]. The reason why there were not consistent results

might be different kinds of tumors and cell lines. But most studies and our results showed miR-494 inhibited cancer. Further studies of the roles of miR-494 in the progress of tumorigenesis are urgently needed.

Silybin was illustrated for several uses such as liver-protective, anti-cancer, anti-inflammation [33]. It inhibited cell proliferation in hepatocarcinoma *in vitro* [34] and *in vivo* [35]. However, the studies of the effects of this drug on OS are very few. In gastric cancer, silybin suppressed MMP-9 [36]. Silybin also inhibited Wnt signaling pathways by decreasing the expression levels of β-catenin [37,38]. Because hsa-miR-494 was regulated by silybin, we further studied its roles in OS. And we revealed silybin inhibited OS cell proliferation. Through hsa-miR-494 we found silybin and studied this traditional drug. We revealed the new effects of silybin on OS. Thus, silybin might be used as a drug treating OS in the future. Further studied are needed to support this statement and explore this drug.

Conflicts of interest

The authors confirm that there are no conflicts of interest.

Author Contributions

The authors made specific contributions as follows: (i) research design: Tianhao Sun; (ii) acquisition, analysis, and interpretation of the data: Tianhao Sun; (iii) drafting of the article: Tianhao Sun; (iv) critical revision of the article: Tianhao Sun and Kelvin S. C. Cheung. (v) funding and other supports: William W. Lu, Zhi-Li Liu, and Frankie Leung.

References

1. Lijie Z, Ranran F, Xiuying L, Yutang H, Bo W, Tao M. Soyasaponin Bb Protects Rat Hepatocytes from Alcohol-Induced Oxidative Stress by Inducing Heme Oxygenase-1. Pharmacogn Mag 2016;12(48):302-306.
2. Chou AJ, Merola PR, Wexler LH et al. Treatment of osteosarcoma at first recurrence after contemporary therapy - The Memorial Sloan-Kettering Cancer Center Experience. Cancer 2005;104(10):2214-2221.
3. Abarrategi A, Tornin J, Martinez-Cruzado L et al. Osteosarcoma: Cells-of-Origin, Cancer Stem Cells, and Targeted Therapies. Stem Cells Int 2016.
4. Zhao L, Zhang JH, Tan HY et al. Gene function analysis in osteosarcoma based on microarray gene expression profiling. Int J Clin Exp Med 2015;8(7):10401-U11667.
5. Rha SY, Kim JH, Roh JK et al. Sequential production and activation of matrix-metalloproteinase-9 (MMP-9) with breast cancer progression. Breast Cancer Res Treat 1997;43(2):175-181.
6. Makarova JA, Shkurnikov MU, Wicklein D et al. Intracellular and extracellular microRNA: An update on localization and biological role. Prog Histochem Cyto 2016;51(3-4):33-49.
7. Sun T, Li CT, Xiong L et al. miR-375-3p negatively regulates osteogenesis by targeting and decreasing the expression levels of LRP5 and beta-catenin. PLoS One 2017;12(2):e0171281.
8. Sun T, Leung F, Lu WW. MiR-9-5p, miR-675-5p and miR-138-5p Damages the Strontium and LRP5-Mediated Skeletal Cell Proliferation, Differentiation, and Adhesion. Int J Mol Sci 2016;17(2):236.
9. Sun MG, Zhou XY, Chen LL et al. The Regulatory Roles of MicroRNAs in Bone Remodeling and Perspectives as Biomarkers in Osteoporosis. Biomed Res Int 2016.

10. Dou CW, Liu ZK, Xu M et al. miR-187-3p inhibits the metastasis and epithelial-mesenchymal transition of hepatocellular carcinoma by targeting S100A4. Cancer Lett 2016;381(2):380-390.

11. Zhang S, Yang Y, Liang ZX et al. Silybin-Mediated Inhibition of Notch Signaling Exerts Antitumor Activity in Human Hepatocellular Carcinoma Cells. Plos One 2013;8(12).

12. Han XF, Wang Z, Wang MY et al. Liver-targeting self-assembled hyaluronic acid-glycyrrhetinic acid micelles enhance hepato-protective effect of silybin after oral administration. Drug Deliv 2016;23(5):1818-1829.

13. Hsieh YS, Chu SC, Yang SF, Chen PN, Liu YC, Lu KH. Silibinin suppresses human osteosarcoma MG-63 cell invasion by inhibiting the ERK-dependent c-Jun/AP-1 induction of MMP-2. Carcinogenesis 2007;28(5):977-987.

14. Cai T, Sun DQ, Duan Y et al. WNT/beta-catenin signaling promotes VSMCs to osteogenic transdifferentiation and calcification through directly modulating Runx2 gene expression. Exp Cell Res 2016;345(2):206-217.

15. Hamidouche Z, Hay E, Vaudin P et al. FHL2 mediates dexamethasone-induced mesenchymal cell differentiation into osteoblasts by activating Wnt/beta-catenin signaling-dependent Runx2 expression. Faseb J 2008;22(11):3813-3822.

16. Wang Q, Yu W, Huang T, Zhu Y, Huang CS. RUNX2 promotes hepatocellular carcinoma cell migration and invasion by upregulating MMP9 expression. Oncology Reports 2016;36(5):2777-2784.

17. Kypta RM, Waxman J. Wnt/beta-catenin signalling in prostate cancer. Nat Rev Urol 2012;9(8):418-428.

18. Masters JR. Cell-line authentication: End the scandal of false cell lines. Nature 2012;492(7428):186.

19. Chatterjee R. Cell biology. Cases of mistaken identity. Science 2007;315(5814):928-931.

20. Shankar J, Messenberg A, Chan J, Underhill TM, Foster LJ, Nabi IR. Pseudopodial actin dynamics control epithelial-mesenchymal transition in metastatic cancer cells. Cancer Res 2010;70(9):3780-3790.

21. Wang T, Wang M, Fang S, Wang Q, Fang R, Chen J. Fibulin-4 is associated with prognosis of endometrial cancer patients and inhibits cancer cell invasion and metastasis via Wnt/beta-catenin signaling pathway. Oncotarget 2017.

22. Colden M, Dar AA, Saini S et al. MicroRNA-466 inhibits tumor growth and bone metastasis in prostate cancer by direct regulation of osteogenic transcription factor RUNX2. Cell Death Dis 2017;8(1):e2572.

23. Fu JJ, Wang S, Lu H et al. In vitro inhibitory effects of terpenoids from Chloranthus multistachys on epithelial-mesenchymal transition via down-regulation of Runx2 activation in human breast cancer. Phytomedicine 2015;22(1):165-172.

24. Gilles C, Polette M, Mestdagt M et al. Transactivation of vimentin by beta-catenin in human breast cancer cells. Cancer Research 2003;63(10):2658-2664.

25. Chang YC, Jan CI, Peng CY, Lai YC, Hu FW, Yu CC. Activation of microRNA-494-targeting Bmi1 and ADAM10 by silibinin ablates cancer stemness and predicts favourable prognostic value in head and neck squamous cell carcinomas. Oncotarget 2015;6(27):24002-24016.

26. Wang J, Shi Q, Yuan TX et al. Matrix metalloproteinase 9 (MMP-9) in osteosarcoma: Review and meta-analysis. Clin Chim Acta 2014;433:225-231.

27. Klein G, Vellenga E, Fraaije MW, Kamps WA, de Bont ESJM. The possible role of matrix metalloproteinase (MMP)-2 and MMP-9 in cancer, e.g. acute leukemia. Crit Rev Oncol Hemat

2004;50(2):87-100.

28. He WL, Li YH, Chen XL et al. miR-494 acts as an anti-oncogene in gastric carcinoma by targeting c-myc. J Gastroen Hepatol 2014;29(7):1427-1434.

29. Zhang R, Chen XN, Zhang SJ et al. Upregulation of miR-494 Inhibits Cell Growth and Invasion and Induces Cell Apoptosis by Targeting Cleft Lip and Palate Transmembrane 1-Like in Esophageal Squamous Cell Carcinoma. Digest Dis Sci 2015;60(5):1247-1255.

30. Liborio-Kimura TN, Jung HM, Chan EKL. miR-494 represses HOXA10 expression and inhibits cell proliferation in oral cancer. Oral Oncol 2015;51(2):151-157.

31. Song LQ, Liu D, Wang BF et al. miR-494 suppresses the progression of breast cancer in vitro by targeting CXCR4 through the Wnt/beta-catenin signaling pathway. Oncology Reports 2015;34(1):525-531.

32. Liu K, Liu SY, Zhang W et al. miR-494 promotes cell proliferation, migration and invasion, and increased sorafenib resistance in hepatocellular carcinoma by targeting PTEN. Oncology Reports 2015;34(2):1003-1010.

33. Polachi N, Bai GR, Li TY et al. Modulatory effects of silibinin in various cell signaling pathways against liver disorders and cancer - A comprehensive review. Eur J Med Chem 2016;123:577-595.

34. Garcia-Maceira P, Mateo J. Silibinin inhibits hypoxia-inducible factor-1 alpha and mTOR/p70S6K/4E-BP1 signalling pathway in human cervical and hepatoma cancer cells: implications for anticancer therapy. Oncogene 2009;28(3):313-324.

35. Cui W, Gu F, Hu KQ. Effects and mechanisms of silibinin on human hepatocellular carcinoma xenografts in nude mice. World J Gastroentero 2009;15(16):1943-1950.

36. Kim S, Choi MG, Lee HS et al. Silibinin Suppresses TNF-alpha-Induced MMP-9 Expression in

Gastric Cancer Cells through Inhibition of the MAPK Pathway. Molecules 2009;14(11):4300-4311.

37. Rajamanickam S, Kaur M, Velmurugan B, Singh RP, Agarwal R. Silibinin Suppresses Spontaneous Tumorigenesis in APC (min/+) Mouse Model by Modulating Beta-Catenin Pathway. Pharm Res-Dordr 2009;26(12):2558-2567.

38. Kaur M, Velmurugan B, Tyagi A, Agarwal C, Singh R, Agarwal R. Silibinin Suppresses Growth of Human Colorectal Carcinoma SW480 Cells in Culture and Xenograft through Down-regulation of beta-Catenin-Dependent Signaling. Neoplasia 2010;12(5):415-424.

Fig. 1 Silence of MMP-9 inhibited OS cell proliferation. (**a**) The relative absorbance of MG-63 cells transfected with a serial dilution of siMMP-9 in the MTT-based colorimetric assay. (**b**) The relative absorbance of Saos-2 cells transfected with a serial dilution of siMMP-9 in the MTT-based colorimetric assay. (**c**) Representative pictures of colonies of MG-63 cells (blue dots) transfected with siMMP-9. (**d**) Quantitation of MG-63 cell colony numbers. (**e**) Representative pictures of colonies of Saos-2 cells transfected with siMMP-9. (**f**) Quantitation of Saos-2 cell colony numbers. (**g**) Relative expression levels of PCNA in MG-63 cells treated with siMMP-9. (**h**) Relative expression levels of PCNA in Saos-2 cells treated with siMMP-9. (**i**) The expression levels of PCNA were compared between siMMP-9-treated cells and controls in MG63 and Saos-2 cells by western blot. β-actin was used as a loading control. * $p < 0.05$, ** $p < 0.01$, n = 3/group.

Fig. 2 Silence of MMP-9 induced OS cell apoptosis. (**a**) The expression levels of PARP1 and Cytochrome C were compared between siMMP-9-treated cells and controls in MG63 and Saos-2 cells. (**b**) TUNEL cell apoptosis assay of MG-63 cells transfected with a serial dilution of siMMP-9 (0, 1.25 nM, and 10 nM). Apoptotic (TUNEL positive) cells were in red. More TUNEL positive (Red) cells were found after the cells were transfected with siMMP-9. With the increase of concentration of siMMP-9, there were more red (apoptosis) cells. (**c**) Quantification of TUNEL positive cells.

Fig. 3 Overexpression of MMP-9 promoted OS cell migration. (**a**) Relative expression levels

of MMP-9 in MMP-9-overexpressed Saos-2 cells and normal Saos-2 cells. (**b**) Representative pictures of MMP-9-overexpressed Saos-2 cells and normal Saos-2 cells. * $p < 0.05$, ** $p < 0.01$, n = 3/group.

Fig. 4 MMP-9 was targeted by hsa-miR-494 which inhibited OS. (**a**) The binding sites between hsa-miR-494 and the 3'UTR of MMP-9. (**b**) The relative luciferase activity of MG-63 cells transfected with luciferase-wild type (or mutant) MMP-9 plasmids and hsa-miR-494 mimics. (**c**) The relative absorbance of MG-63 cells transfected with hsa-miR-494 inhibitors in the XTT-based colorimetric assay. (**d**) The relative absorbance of Saos-2 cells transfected with hsa-miR-494 inhibitors in the XTT-based colorimetric assay. (**e**) The expression levels of caspase-3 were compared between hsa-miR-494 mimics or inhibitors-treated cells and controls in MG-63 and Saos-2 cells by western blot. (**f**) The expression levels of β-catenin/RUNX2/vimentin were compared between hsa-miR-494-treated cells and controls in MG-63 and Saos-2 cells by western blot. * $p < 0.05$. n =3/group.

Fig. 5 Hsa-miR-494 were upregulated by silybin which inhibited OS cell proliferation. (**a**) Expression levels of hsa-miR-494 in Saos-2 cells upon silybin treatment. (**b**) Representative pictures of colonies of MG-63 and Saos-2 cells treated with silybin (20 μM and 80 μM). (**c**) Quantitation of colony numbers of MG-63 cells treated with silybin. (**d**) Quantitation of colony numbers of Saos-2 cells treated with silybin. (**e**) The relative absorbance of MG-63 cells treated with a serial dilution of silybin in the XTT-based colorimetric assay. (**f**) The relative absorbance of Saos-2 cells transfected with a serial dilution of silybin in the XTT-based colorimetric assay.

$p < 0.05$. ** $p < 0.01$, n =3/group.

Fig. 6 Silybin modulated the protein levels of β-catenin and RUNX2. (**a**) The expression levels of β-catenin and RUNX2 were compared between DMSO and silybin-treated cells in MG-63 (left panel) or Saos-2 cells (right panel) by western blot analysis. β-actin was used as a loading control. (**b**) Representative staining images of Saos-2 cells. The intensity and the degree of green represented the expression levels of RUNX2. After treatment of silybin, the cells were greener. In other words, the degree of green was higher in the silybin-treated group than the control group. More green cells were found after the cells were treated with silybin. (**c**) Quantification of the intensity of fluorescence.

Fig. 7 The flowchart of the main study factors and their relationships.

Table 1. Sequences of all primers

Primer Name	Sequences (5'–3')
GAPDH (homo sapiens) Forward	ATTGTCAGCAATGCATCCTG
GAPDH (homo sapiens) Reverse	ATGGACTGTGGTCATGAGCC
PCNA (homo sapiens) Forward	CTGTGTAGTAAAGATGCC
PCNA (homo sapiens) Reverse	TCCATTTCCAAGTTCTCC
MMP-9 (homo sapiens) Forward	AACCAATCTCACCGACAGG
MMP-9 (homo sapiens) Reverse	CGACTCTCCACGCATCTC
U6 (RNU6B) Forward	ATGACACGCAAATTCGTGAAGC
hsa-miR-494 Forward	UGAAACATACACGGGAAACCTC
miRNAs Reverse	GCGAGCACAGAATTAATACGAC

Table 2. STR loci data comparison of MG-63 and Saos-2

	MG-63		Saos-2	
STR locus names	Standard (ATCC CRL-1427)	Query Results (Our Cell)	Standard (ATCC HTB-85)	Query Results (Our Cell)
AmeL	X,Y	X,Y	X,X	X,X
TH01	9.3,9.3	9.3,9.3	6,9	6,9
D5S818	11,12	11,12	12,12	12,12
D13S317	11,11	11,11	12,13	12,13
D7S820	10,10	10,10	8,10	8,10
D16S539	11,11	11,11	12,13	12,13
CSFIPO	10,12	10,12	10,10	10,10
vWA	16,19	16,19	18,18	18,18
TPOX	8,11	8,11	8,8	8,8

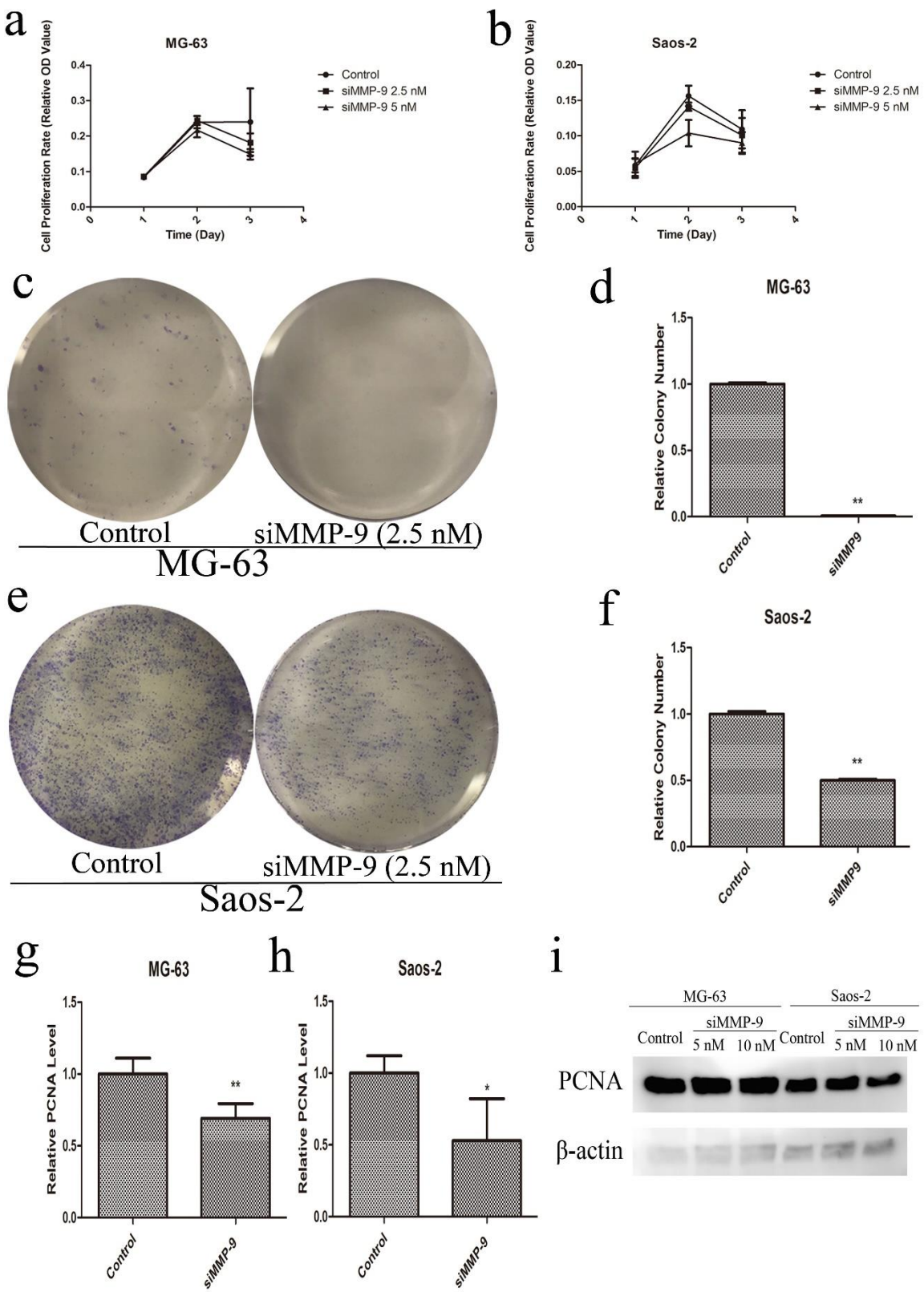
a
MG-63
Cell Proliferation Rate (Relative OD Value)
Time (Day)
Control
siMMP-9 2.5 nM
siMMP-9 5 nM
b
Saos-2
Cell Proliferation Rate (Relative OD Value)
Time (Day)
Control
siMMP-9 2.5 nM
siMMP-9 5 nM
c
Control
siMMP-9 (2.5 nM)
MG-63
d
MG-63
Relative Colony Number
**
Control
siMMP9
e
Control
siMMP-9 (2.5 nM)
Saos-2
f
Saos-2
Relative Colony Number
**
Control
siMMP9
g
MG-63
Relative PCNA Level
**
Control
siMMP-9
h
Saos-2
Relative PCNA Level
*
Control
siMMP-9
i
MG-63
Saos-2
Control
siMMP-9
5 nM
10 nM
Control
siMMP-9
5 nM
10 nM
PCNA
β-actin

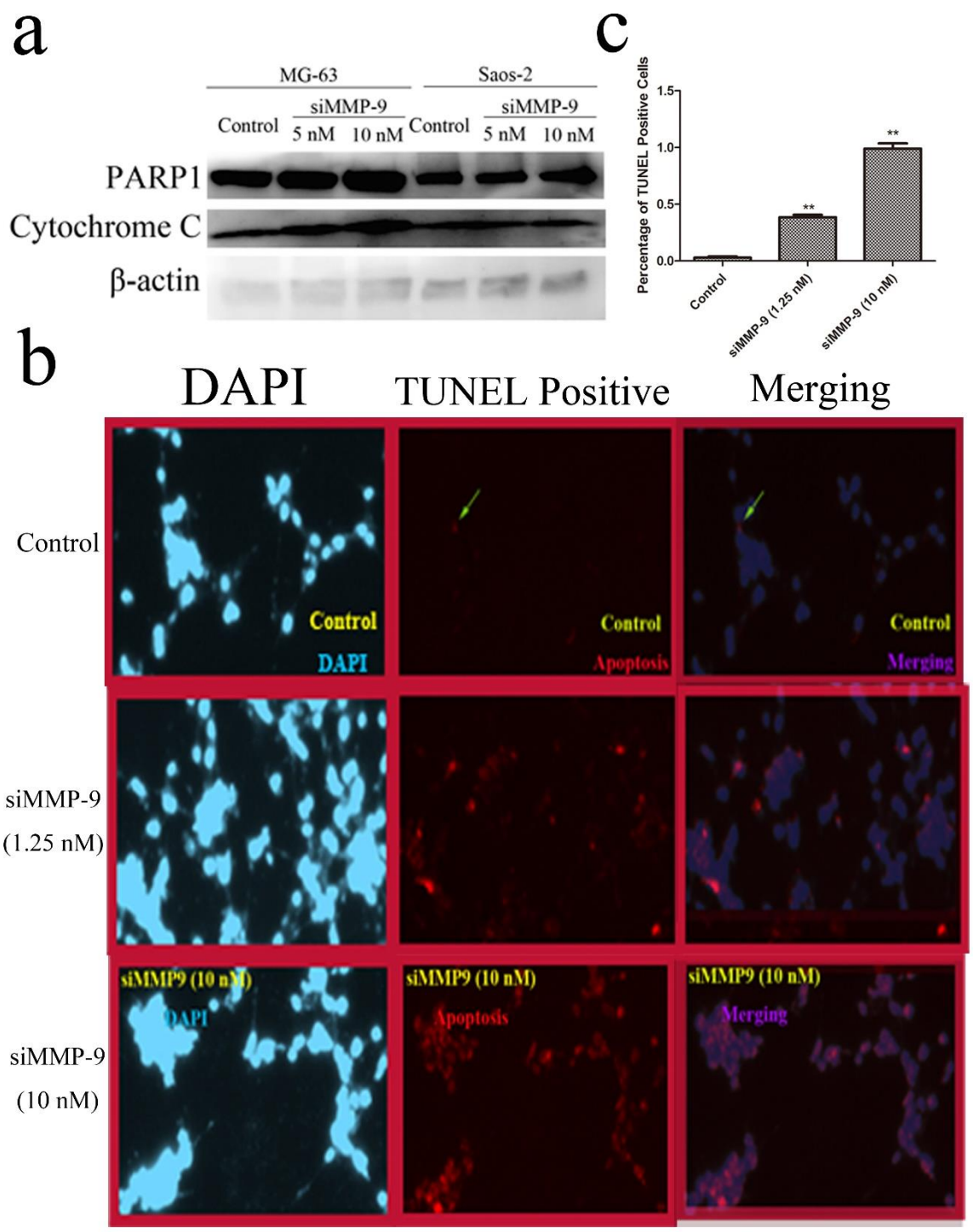
a
MG-63
Saos-2
Control
siMMP-9
5 nM
10 nM
Control
siMMP-9
5 nM
10 nM
PARP1
Cytochrome C
β-actin
c
Percentage of TUNEL Positive Cells
1.5
1.0
0.5
0.0
**
**
Control
siMMP-9 (1.25 nM)
siMMP-9 (10 nM)
b
DAPI
TUNEL Positive
Merging
Control
siMMP-9
(1.25 nM)
siMMP-9
(10 nM)
Control
DAPI
Control
Apoptosis
Control
Merging
siMMP9 (10 nM)
DAPI
siMMP9 (10 nM)
Apoptosis
siMMP9 (10 nM)
Merging

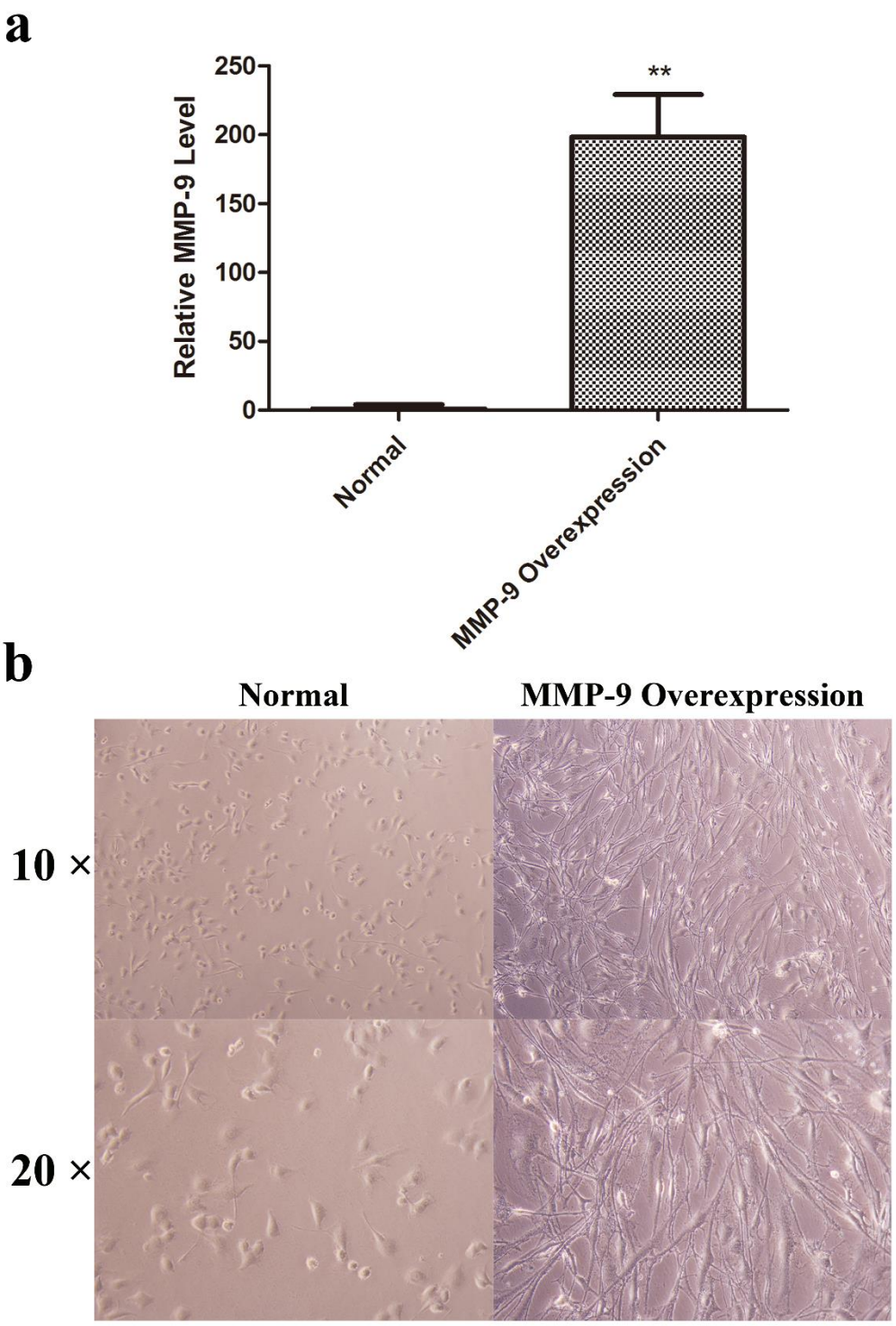
a
Relative MMP-9 Level
250
200
150
100
50
0
**
Normal
MMP-9 Overexpression
b
Normal
MMP-9 Overexpression
10 ×
20 ×

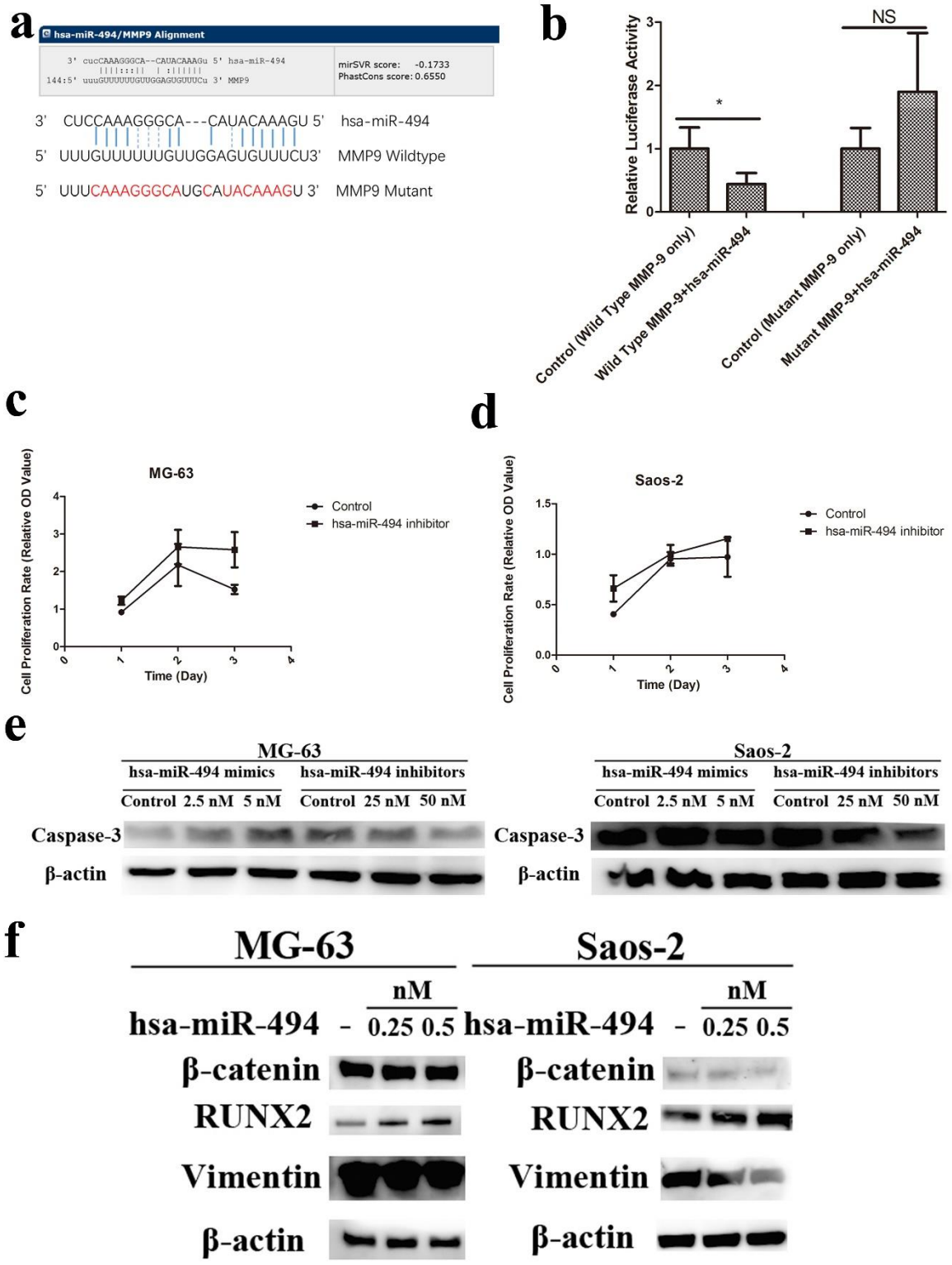
a
hsa-miR-494/MMP9 Alignment
mirSVR score: -0.1733
PhastCons score: 0.6550
3' CUCCAAAGGGCA---CAUACAAAGU 5' hsa-miR-494
5' UUUGUUUUUUGUUGGAGUGUUUCU3' MMP9 Wildtype
5' UUUCAAAGGGCAUGCAUACAAAGU 3' MMP9 Mutant
b
Relative Luciferase Activity
NS
*
Control (Wild Type MMP-9 only)
Wild Type MMP-9+hsa-miR-494
Control (Mutant MMP-9 only)
Mutant MMP-9+hsa-miR-494
c
MG-63
Cell Proliferation Rate (Relative OD Value)
Time (Day)
Control
hsa-miR-494 inhibitor
d
Saos-2
Cell Proliferation Rate (Relative OD Value)
Time (Day)
Control
hsa-miR-494 inhibitor
e
MG-63
hsa-miR-494 mimics
hsa-miR-494 inhibitors
Control 2.5 nM 5 nM Control 25 nM 50 nM
Caspase-3
β-actin
Saos-2
hsa-miR-494 mimics
hsa-miR-494 inhibitors
Control 2.5 nM 5 nM Control 25 nM 50 nM
Caspase-3
β-actin
f
MG-63
nM
hsa-miR-494 - 0.25 0.5
β-catenin
RUNX2
Vimentin
β-actin
Saos-2
nM
hsa-miR-494 - 0.25 0.5
β-catenin
RUNX2
Vimentin
β-actin

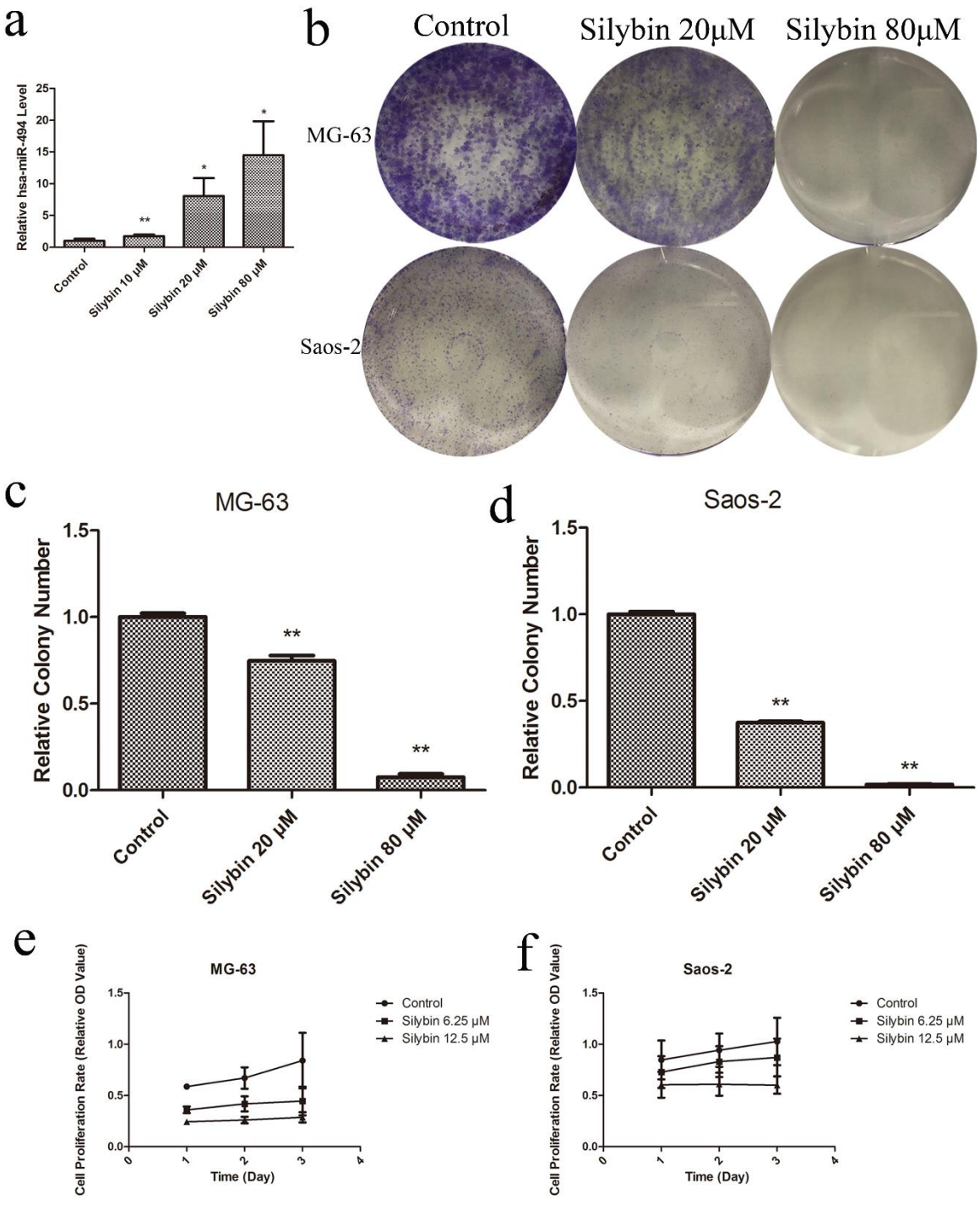
a
Relative hsa-miR-494 Level
25
20
15
10
5
0
**
*
*
Control
Silybin 10 μM
Silybin 20 μM
Silybin 80 μM
b
Control
Silybin 20μM
Silybin 80μM
MG-63
Saos-2
c
MG-63
Relative Colony Number
1.5
1.0
0.5
0.0
**
**
Control
Silybin 20 μM
Silybin 80 μM
d
Saos-2
Relative Colony Number
1.5
1.0
0.5
0.0
**
**
Control
Silybin 20 μM
Silybin 80 μM
e
MG-63
Cell Proliferation Rate (Relative OD Value)
1.5
1.0
0.5
0.0
0
1
2
3
4
Time (Day)
Control
Silybin 6.25 μM
Silybin 12.5 μM
f
Saos-2
Cell Proliferation Rate (Relative OD Value)
1.5
1.0
0.5
0.0
0
1
2
3
4
Time (Day)
Control
Silybin 6.25 μM
Silybin 12.5 μM

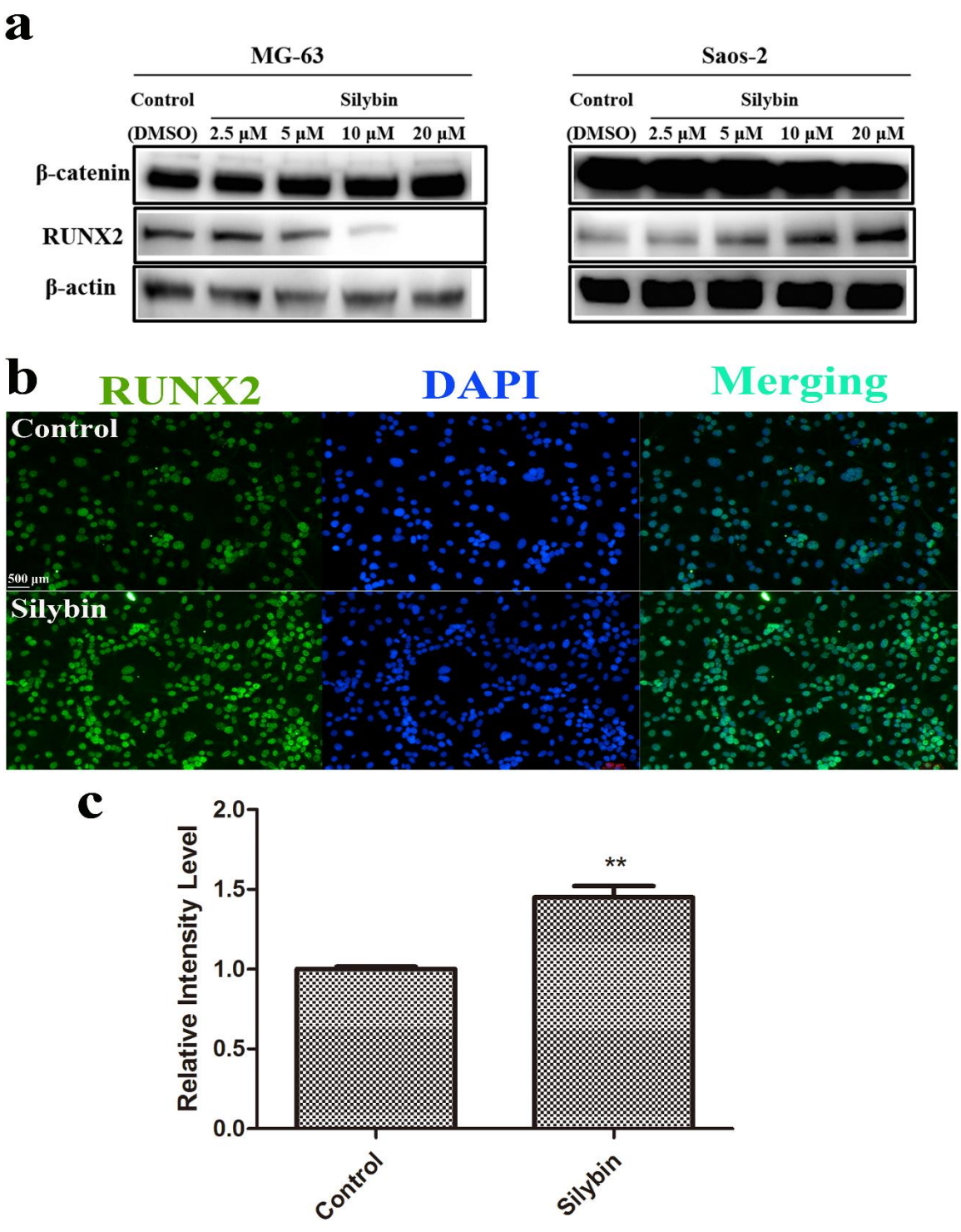
a
MG-63
Saos-2
Control
(DMSO)
Silybin
2.5 μM
5 μM
10 μM
20 μM
β-catenin
RUNX2
β-actin
b
RUNX2
DAPI
Merging
Control
Silybin
500 μm
c
Relative Intensity Level
2.0
1.5
1.0
0.5
0.0
**
Control
Silybin

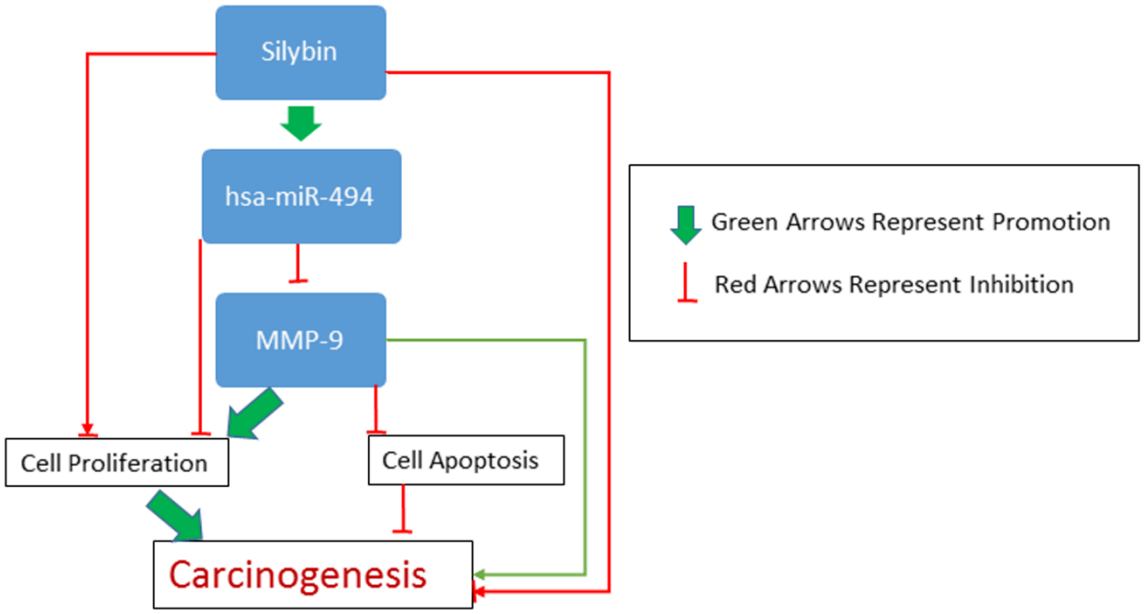
Silybin
hsa-miR-494
MMP-9
Cell Proliferation
Cell Apoptosis
Carcinogenesis
Green Arrows Represent Promotion
Red Arrows Represent Inhibition

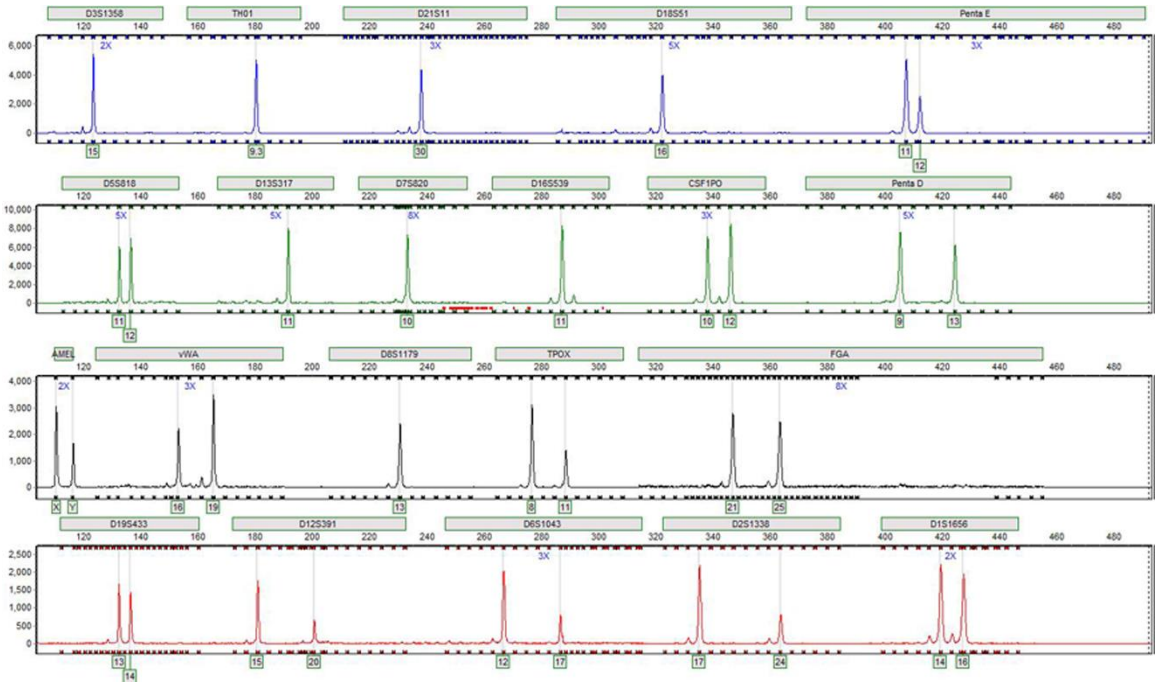

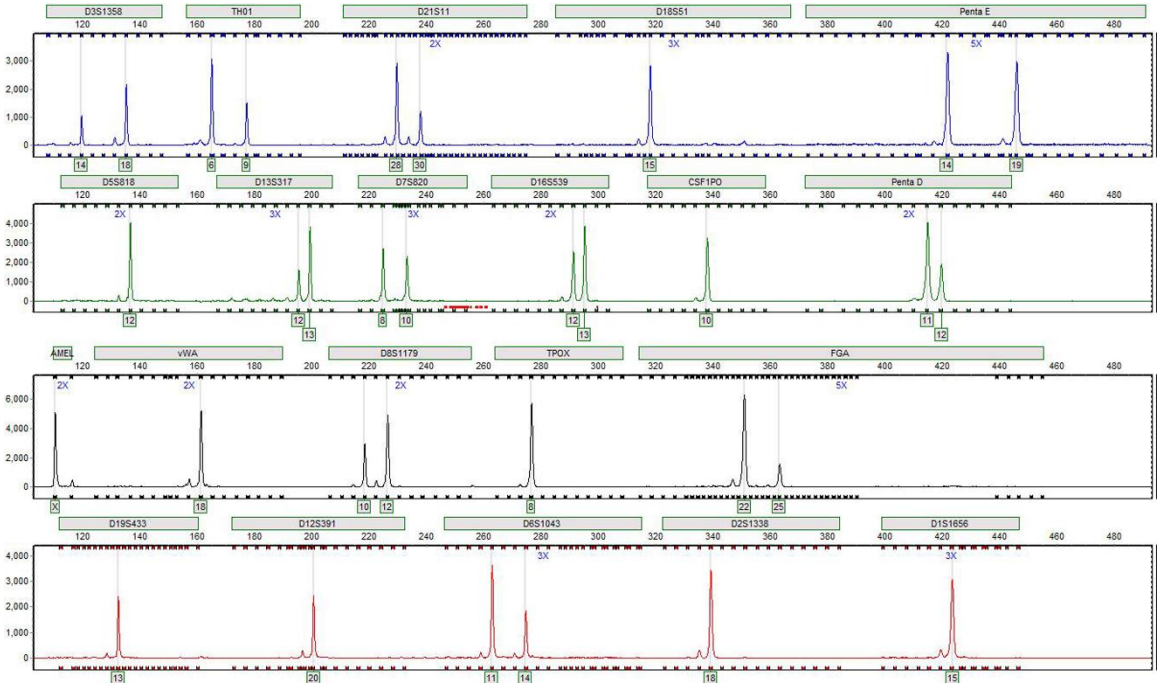
D3S1358
TH01
D21S11
D18S51
Penta E
D5S818
D13S317
D7S820
D16S539
CSF1PO
Penta D
AMEL
vWA
D8S1179
TPOX
FGA
D19S433
D12S391
D6S1043
D2S1338
D1S1656